A Bearings-Only Trajectory Shaping Guidance Law With Look-Angle Constraint

YASH RAJ SHARMA
ASHWINI RATNOO
Indian Institute of Science, Bangalore, India

This paper addresses the problem of achieving a desired impact angle against a stationary target with seeker's field-of-view limits. A bearings-only information based guidance law is investigated as a prospective solution. Analyzing the look-angle and the line-of-sight angle relationship, closed-form expressions of the guidance gains are derived for the desired impact angle and maximum look-angle constraints. A detailed analysis is carried out for lateral acceleration boundedness resulting in a design solution expressed in impact angle-maximum look angle space. Validating the guidance law, numerical simulations are performed using a kinematic vehicle model and a realistic model with given thrust and aerodynamic characteristics. Overall, the work offers an easily implementable guidance method with simple structure and closed-form guidance gains.

Manuscript received August 29, 2018; revised December 27, 2018; released for publication March 1, 2019. Date of publication March 27, 2019; date of current version December 5, 2019.

DOI. No. 10.1109/TAES.2019.2906090

Refereeing of this contribution was handled by C.-K. Ryoo.

Authors' address: Y. R. Sharma and A. Ratnoo are with the Department of Aerospace Engineering, Indian Institute of Science, Bangalore 560012, India, E-mail: (yashrajbasti@gmail.com; ratnoo@iisc.ac.in). *(Corresponding author: Yash Raj Sharma.)*

I. INTRODUCTION

Maintaining seeker lock-on to the target is a primary requirement for any prospective guidance law. Shaping the vehicle trajectory to satisfy a terminal impact angle becomes challenging, particularly for a missile seeker with a narrow field-of-view.

Impact angle control is a widely investigated topic in the guidance literature. The angle is defined as the terminal heading direction along which a missile hits the target and is important for improving warhead effectiveness and lethality. Kim and Grider [1] introduced a suboptimal guidance law for re-entry vehicles with a constraint on the body attitude angle at impact. An optimal impact angle control guidance law against moving targets with time varying missile velocities was proposed by Song *et al.* [2]. Ryoo *et al.* [3] presented an optimal guidance law, which uses a linear combination of the ramp and step acceleration responses of the missile satisfying the desired terminal impact angle. An extension of that work was presented in [4] as a solution to linear quadratic optimal control problem with the energy cost weighted by a power of the time-to-go. Oza and Padhi [5] presented a nonlinear suboptimal guidance law for air-to-ground missiles satisfying the impact angle. Shaferman and Shima [6] derived impact angle constrained guidance laws using optimal control and differential game theories for imposing a terminal intercept angle against a target. Later, Shima [7] proposed an impact angle guidance method for aerial engagement scenarios intercepting a target with all possible attack geometries. Sliding mode control was proposed for the implementation of that guidance law. Another sliding mode control based guidance law was proposed by Kumar *et al.* [8] for the interception of targets satisfying impact angle constraint.

Proportional navigation (PN) and its variants present a popular and extensively used guidance framework addressing a variety of applications. An adaptive PN guidance approach is used by Lu *et al.* [9] for guiding a hypersonic lifting vehicle satisfying the terminal impact angle against a stationary target. Ratnoo and Ghose [10] proposed a two stage guidance law achieving desired impact angles against stationary targets. In that work, a lower navigation gain is used in the first stage to orient the trajectory, followed by a higher navigation gain to achieve desired impact angles. Adding a constant bias term to the pure PN guidance command, Erer and Merttopcuoglu [11] presented another impact angle constrained guidance law. Recently, Ratnoo [12] proposed a nonswitching guidance law, which presents a guidance command derived using the product of line-of-sight angle and line-of-sight rate. However, the works [1]–[12] did not consider seeker's field-of-view limit while deriving the guidance law addressing the impact angle constraint.

The problem of impact angle constrained guidance with seeker field-of-view constraint has received significant interest over the last decade. Erer *et al.* [13] developed two switched gain guidance schemes based on biased pure PN and unbiased PN for satisfying impact angle as well as

look-angle constraints. Tekin and Erer [14] analyzed in detail a switched PN-based guidance method for impact angle control satisfying physical constraints, namely, seeker field-of-view limit, and the lateral acceleration capability. Therein, the guidance gains are numerically computed for the midphase and terminal phase of the engagement. Kim *et al.* [15] presented a switched bias augmented PN guidance law, wherein, the switch in bias terms is utilized for maintaining seeker look angle constraint. The method was further developed for nonmaneuvering moving targets in [16]. Two-stage PN guidance law introduced in [10] was analyzed for look-angle constraints by Ratnoo [17]. He and Lin [18] proposed a sliding mode control based impact angle constrained guidance method with seeker's field-of-view limit. That work utilizes a switching, which adds an additional term to the guidance law for maintaining seeker's lock on to the target. Park *et al.* [19] proposed a three-phased impact angle control guidance based on the optimal control theory. The work involves range information based switching logic between different guidance phases. Driving the terminal lateral acceleration to zero, an approach similar to [19] was used in [20] by considering a range-to-go weighted performance index. It is noteworthy that the works in [13]–[20] rely on switching of guidance command corresponding to discontinuity in the lateral acceleration, which may be undesirable from an implementation point of view.

With seeker's field-of-view limits, a two biased augmented PN guidance method was proposed by Yang *et al.* [21]. Therein, the first term keeps the seeker's lock-on during the engagement, and the second term ensures the terminal impact angle. The guidance law uses an online recursive switching condition for changing the bias terms, and that requires additional computations for duration and/or the magnitude of bias terms. More recently, Kim *et al.* [22] presented a bearings information guidance law derived from the sliding mode theory for impact angle control with prescribed seeker's field-of-view limits. Therein, a sigmoid function was used in the sliding surface to limit the magnitude of seeker's look angle.

As the main contribution of this paper, a bearings-only guidance law is investigated for achieving desired impact angles considering seeker's field-of-view limits. Imposing the maximum look-angle and the impact angle as design constraints, closed-form expressions are derived for the guidance gains. Capturability of the proposed guidance law is guaranteed by proving strictly reducing heading error in the terminal phase of the engagement. Boundedness of the terminal lateral acceleration is ascertained by analyzing the effective time varying navigation gain and imposing a condition on its terminal value. This results in a design space region in which the guidance law can be used. Simulation results present the efficacy of the guidance law. A similar structure of the guidance law was used in [23] for mimicking short range ballistic trajectories. Therein, the gains essentially depend on matching the initial heading error rates of the guided trajectory and the ballistic one. It is noteworthy that the generic two-gain form of the guidance law can be applied to a variety of applications. This work analyzes the guidance law for impact angle constrained interception of targets without violating seeker's field-of-view limits.

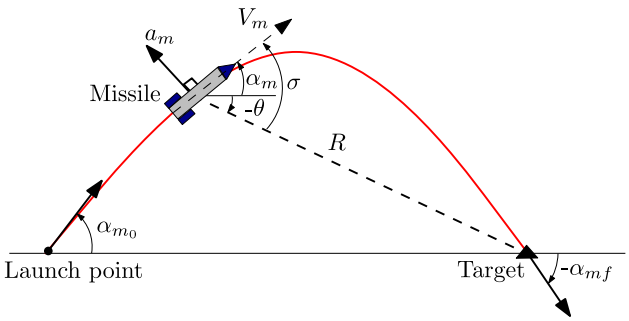

Fig. 1. Engagement scenario.

The remainder of the paper is organized as follows: The guidance problem is formulated in Section II. Section III discusses the guidance law, and its impact angle and the look-angle characteristics. Capturability and lateral acceleration boundedness is analyzed in Section IV. Simulation results are presented in Section V and concluding remarks are offered in Section VI.

II. PROBLEM FORMULATION

Consider a planar surface-to-surface engagement scenario between a missile and a target as shown in Fig. 1. As expressed in a fixed reference frame, the missile heading is denoted by α_m. The line-of-sight separation and the line-of-sight angle are denoted by R and θ, respectively. Lateral acceleration a_m is the commanded guidance input, which is applied normal to the missile velocity V_m. The nonlinear engagement kinematics can be expressed in a polar form as

$$\dot{R} = -V_m \cos(\alpha_m - \theta) \tag{1}$$

$$\dot{\theta} = \frac{-V_m \sin(\alpha_m - \theta)}{R} \tag{2}$$

$$\dot{\alpha}_m = \frac{a_m}{V_m} \tag{3}$$

For surface-to-surface engagements, the launch angle of missile is bounded by

$$\alpha_{m_0} \in (0,\ \pi) \tag{4}$$

Assuming negligible angles of attack, the seeker look-angle σ can be expressed as

$$\sigma = \alpha_m - \theta \tag{5}$$

The objective here is to generate a guidance command, which, at the final time t_f, leads to

$$\lim_{t \to t_f} R = \lim_{t \to t_f} (\alpha_m - \alpha_{m_f}) = 0 \tag{6}$$

while satisfying

$$\sigma(t) \in [-\sigma_{\max},\ \sigma_{\max}] \tag{7}$$

where α_{m_f} denotes the desired impact angle

$$\alpha_{m_f} \in [-\pi,\ 0] \tag{8}$$

and $\sigma_{\max}$ represents the maximum look-angle of the missile seeker.

III. GUIDANCE DESIGN

This section presents a bearings-only guidance law and analyzes its impact angle and look-angle characteristics.

A. Guidance Law

Consider a bearings-only information based guidance law as

$$a_m = (k_1 - k_2\theta)\dot{\theta} V_m \tag{9}$$

where k_1 and k_2 are the guidance gains, which are subsequently determined by imposing the impact angle and maximum look-angle constraints. As given in (9), the term $(k_1 - k_2\theta)$ provides time varying nature to the overall guidance gain and facilitates imposing two additional guidance objectives. The overall guidance gain has a monotonic variation of the line-of-sight angle. Also, as will be shown in Section IV-B, the proposed variation also leads to satisfying the terminal lateral acceleration boundedness.

B. Impact Angle Characteristics

Using (3) and (9), the missile turning rate can be expressed as

$$\dot{\alpha}_m = (k_1 - k_2\theta)\dot{\theta} \tag{10}$$

Integrating (10), the resulting missile heading can be obtained as

$$\alpha_m = k_1\theta - \frac{k_2\theta^2}{2} + C \tag{11}$$

where C is an arbitrary constant that can be deduced using the initial conditions as

$$C = \alpha_{m_0} - k_1\theta_0 + \frac{k_2\theta_0^2}{2} \tag{12}$$

where α_{m_0} and θ_0 denote the initial heading angle and the initial line-of-sight angle, respectively. For surface-to-surface engagement scenarios, the initial line-of-sight angle is $\theta_0 = 0$. Using this information in (12), the constant C is determined as $C = \alpha_{m_0}$, which upon substitution in (11) leads to

$$\alpha_m = k_1\theta - \frac{k_2\theta^2}{2} + \alpha_{m_0} \tag{13}$$

Against stationary targets, the collision course corresponds to

$$\alpha_{m_f} = \theta_f \tag{14}$$

where θ_f corresponds to the terminal value of the line-of-sight angle. Using (13) in (14) at final time, leads to

$$\alpha_{m_f} = k_1\alpha_{m_f} - \frac{k_2\alpha_{m_f}^2}{2} + \alpha_{m_0} \tag{15}$$

Satisfying a given impact angle, a relationship between the gains k_1 and k_2 can be deduced by rearranging (15) as

$$k_2 = \frac{(2k_1 - 2)\alpha_{m_f} + 2\alpha_{m_0}}{\alpha_{m_f}^2} \tag{16}$$

C. Look-Angle Characteristics

Using (5) and (13), the look-angle can be expressed as

$$\sigma = k_1\theta - \frac{k_2\theta^2}{2} + \alpha_{m_0} - \theta$$

$$\Rightarrow \sigma = (k_1 - 1)\theta - \frac{k_2\theta^2}{2} + \alpha_{m_0} \tag{17}$$

Differentiating (17) with respect to the line-of-sight angle θ leads to

$$\frac{d\sigma}{d\theta} = (k_1 - 1) - k_2\theta \tag{18}$$

On imposing $\frac{d\sigma}{d\theta} = 0$ in (18), the line-of sight angle at the maximum look-angle can be derived as

$$\theta_{\sigma_{\max}} = \frac{k_1 - 1}{k_2} \tag{19}$$

Using (17) and (19), the maximum look-angle can be deduced as

$$\sigma_{\max} = (k_1 - 1)\left(\frac{k_1 - 1}{k_2}\right) - \left(\frac{k_2}{2}\right)\left(\frac{k_1 - 1}{k_2}\right)^2 + \alpha_{m_o}$$

$$\Rightarrow \sigma_{\max} = \frac{(k_1 - 1)^2}{2k_2} + \alpha_{m_0} \tag{20}$$

For the target to be inside the seeker's field-of-view at the beginning of the engagement

$$\sigma(t_0) \geq \alpha_{m_0} \tag{21}$$

Hence, any design $\sigma_{\max}$ is lower bounded by

$$\sigma_{\max} \geq \alpha_{m_o} \tag{22}$$

Using (22) in (20), and considering a finite $\sigma_{\max}$ leads to

$$k_2 > 0 \tag{23}$$

In a surface-to-surface engagement scenario, the line-of-sight angle varies as

$$\theta \in [-\pi,\ 0] \tag{24}$$

Consequently, using (19), (23), and (24), the condition on the guidance gain k_1 for a realizable $\theta_{\sigma_{\max}}$ can be deduced as

$$k_1 \leq 1 \tag{25}$$

The minimum value of the look-angle is at the interception, that is, at $t = t_f$

$$\sigma(t_f) = 0 \tag{26}$$

D. Feasible Guidance Gains

The idea here is to impose the maximum look-angle as additional design constraint, and use that relation together with (16) to deduce the guidance gains. Considering $\sigma_{\max}$ to be the desired maximum look-angle, and rearranging (20)

$$2k_2\sigma_{\max} = (k_1 - 1)^2 + 2k_2\alpha_{m_0}$$

$$\Rightarrow 2k_2(\sigma_{\max} - \alpha_{m_0}) = (k_1 - 1)^2 \tag{27}$$

Using (16) in (27) yields

$$4(\sigma_{\max}-\alpha_{m_0})\left(\frac{(2k_1-2)\alpha_{m_f}+2\alpha_{m_0}}{\alpha_{m_f}^2}\right)=(k_1-1)^2 \tag{28}$$

which upon further simplification results in

$$\begin{aligned}&4(k_1-1)\left(\frac{\sigma_{\max}-\alpha_{m_0}}{\alpha_{m_f}}\right)+\frac{4\alpha_{m_0}}{\alpha_{m_f}}\left(\frac{\sigma_{\max}-\alpha_{m_0}}{\alpha_{m_f}}\right)\\&\quad=(k_1-1)^2\\&\Rightarrow(k_1-1)^2-4\left(\frac{\sigma_{\max}-\alpha_{m_0}}{\alpha_{m_f}}\right)(k_1-1)\\&\quad-\frac{4\alpha_{m_0}}{\alpha_{m_f}}\left(\frac{\sigma_{\max}-\alpha_{m_0}}{\alpha_{m_f}}\right)=0\\&\Rightarrow(k_1-1)^2-\beta(k_1-1)-\beta\frac{\alpha_{m_0}}{\alpha_{m_f}}=0\end{aligned} \tag{29}$$

where

$$\beta=\frac{4(\sigma_{\max}-\alpha_{m_0})}{\alpha_{m_f}} \tag{30}$$

Using (8), (22), and (30) results in

$$\beta\le 0 \tag{31}$$

Algebraic roots of (29) can be deduced as

$$k_1=\frac{\beta\pm\sqrt{\beta^2+4\beta\frac{\alpha_{m_0}}{\alpha_{m_f}}}}{2}+1 \tag{32}$$

Since, $\alpha_{m0}>0$ and $\alpha_{m_f}<0$, the value of gain $k_1=\frac{\beta+\sqrt{\beta^2+4\beta\frac{\alpha_{m_0}}{\alpha_{m_f}}}}{2}+1$ violates (25) for $\beta<0$, and is hence discarded. Consequently, the feasible guidance gains are obtained using (16) and (32) as

$$k_1=\frac{\beta-\sqrt{\beta^2+4\beta\frac{\alpha_{m_0}}{\alpha_{m_f}}}}{2}+1 \tag{33}$$

and

$$k_2=\frac{\alpha_{m_f}\left(\beta-\sqrt{\beta^2+4\beta\frac{\alpha_{m_0}}{\alpha_{m_f}}}\right)+2\alpha_{m_0}}{\alpha_{m_f}^2} \tag{34}$$

In addition, $\beta=0$ is a limiting case, which using (30), (33), and (34) corresponds to

$$\sigma_{\max}=\alpha_{m_0},\ k_1=1,\ k_2=\frac{2\alpha_{m_0}}{\alpha_{m_f}} \tag{35}$$

Considering a specific maximum look-angle of $\sigma_{\max}=60^\circ$ and an impact angle $\alpha_{m_f}=-90^\circ$, Fig. 2 shows the typical variation in guidance gains k_1 and k_2 with different launch angles.

IV. ANALYSIS OF THE GUIDANCE LAW

This section analyzes the capturability and the terminal lateral acceleration characteristics of the proposed guidance law.

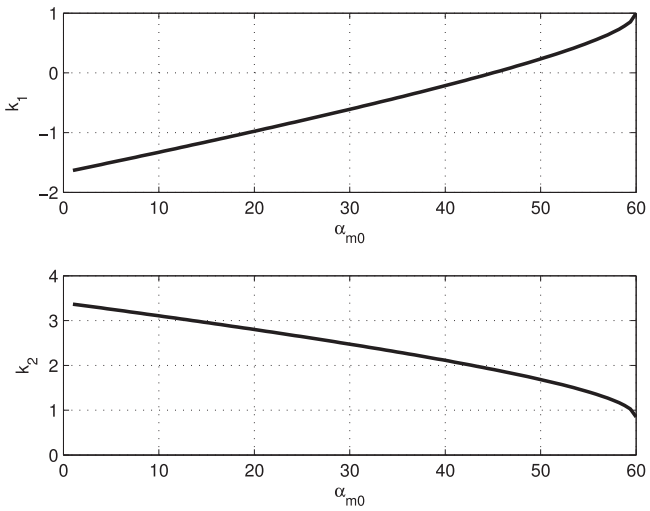

Fig. 2. Typical variation in guidance gains for $\sigma_{\max}=60^\circ$, and $\alpha_{m_f}=-90^\circ$.

A. Capturability

Target interception is a fundamental requirement for any missile guidance law. A strictly reducing heading error variation in the terminal phase of the engagement guarantees successful interception of the target. The heading error rate can also be expressed as

$$\frac{d\sigma}{dt}=\frac{d\sigma}{d\theta}\frac{d\theta}{dt} \tag{36}$$

Using (18), (19), (23), and (25), the variation in heading error with line-of-sight angle θ is governed by

$$\frac{d\sigma}{d\theta}\begin{cases}<0 & \theta>\theta_{\sigma_{\max}}\\=0 & \theta=\theta_{\sigma_{\max}}\\>0 & \theta<\theta_{\sigma_{\max}}\end{cases} \tag{37}$$

From (37), it is evident that the heading error of the missile increases with line-of-sight angle in the terminal phase ($\theta<\theta_{\sigma_{\max}}$). Also, using (2), the line-of-sight rate can be expressed as

$$\dot\theta=\frac{-V_m\sin\sigma}{R} \tag{38}$$

Since

$$\sigma\in(0,\ \pi) \tag{39}$$

Using (38) in (39) leads to

$$\dot\theta<0 \tag{40}$$

Using (36), (37), and (40)

$$\frac{d\sigma}{dt}<0,\ \theta<\theta_{\sigma_{\max}} \tag{41}$$

Hence, using (26) and (41), the heading error σ strictly decreases in the terminal phase $\left(\theta<\theta_{\sigma_{\max}}\right)$ leading to interception at $\theta=\alpha_{m_f}$.

B. Terminal Lateral Acceleration Characteristics

Since, the lateral acceleration capability of a missile is limited, it is critical to ascertain the boundedness of the guidance command. The guidance law of (9) can be rewritten in a form resembling PN as

$$\dot{\alpha}_m = N(t)\dot{\theta}$$

where $N(t)$ is the time varying effective navigation gain expressed as

$$N(t) = k_1 - k_2\theta \tag{42}$$

Differentiating (42) with respect to the line-of-sight angle θ results in

$$\frac{dN}{d\theta} = -k_2 \tag{43}$$

Using (23) in (43) leads to

$$\frac{dN}{d\theta} < 0 \tag{44}$$

The time derivative of the effective navigation gain N can be expressed as

$$\frac{dN}{dt} = \frac{dN}{d\theta}\frac{d\theta}{dt} \tag{45}$$

Using (38) and (44) in (45) yields

$$\frac{dN}{dt} > 0 \tag{46}$$

Governed by (46), the effective navigation gain of the proposed guidance law is a strictly increasing function of time. Classical results on PN [24] ascertain the boundedness of the terminal lateral acceleration for navigation gains satisfying

$$N \geq 2 \tag{47}$$

It is noteworthy from (2) that the line-of-sight rate can go unbounded only at the time of interception as $R \to 0$. Consequently, the boundedness of lateral acceleration can be ascertained solely by analyzing the effective navigation gain in the terminal phase near interception. Accordingly, evaluating the effective navigation gain at the final time t_f by using (14) and (42) in (47) results in

$$N(t_f) = k_1 - k_2\alpha_{m_f} \geq 2 \tag{48}$$

Furthermore, using (16) in (48) leads to

$$k_1 - \left(\frac{(2k_1 - 2)\alpha_{m_f} + 2\alpha_{m_0}}{\alpha_{m_f}^2}\right)\alpha_{m_f} \geq 2$$

$$\Rightarrow k_1 \leq \frac{-2\alpha_{m_0}}{\alpha_{m_f}} \tag{49}$$

Using (33) in (49) leads to

$$\frac{\beta - \sqrt{\beta^2 + 4\beta\frac{\alpha_{m_0}}{\alpha_{m_f}}}}{2} + 1 \leq \frac{-2\alpha_{m_0}}{\alpha_{m_f}}$$

$$\Rightarrow (\beta + 2) + \frac{4\alpha_{m_0}}{\alpha_{m_f}} \leq \sqrt{\beta^2 + 4\beta\frac{\alpha_{m_0}}{\alpha_{m_f}}} \tag{50}$$

The left-hand side of inequality (50) can take positive or negative signs. Accordingly, the rest of the analysis is consolidated as Propositions 1 and 2.

PROPOSITION 1 Using the proposed guidance law, all impact angles $\alpha_{m_f} \in [-2\alpha_{m_0}, 0]$ can be achieved with a bounded lateral acceleration for any design $\sigma_{\max}$ satisfying $\sigma_{\max} \geq \alpha_{m_0}$.

PROOF Let

$$\delta = (\beta + 2) + \frac{4\alpha_{m_0}}{\alpha_{m_f}} \tag{51}$$

Since, nonpositive values of δ inherently satisfy (50). Using $\delta \leq 0$ in (51) implies

$$(\beta + 2) + \frac{4\alpha_{m_0}}{\alpha_{m_f}} \leq 0$$

$$\Rightarrow (2 + \beta) \leq \frac{-4\alpha_{m_0}}{\alpha_{m_f}} \tag{52}$$

Using (30) in (52) yields

$$\sigma_{\max} \geq \frac{-\alpha_{m_f}}{2}, \delta \leq 0 \tag{53}$$

Furthermore, using (22), (53) holds if

$$\alpha_{m_0} \geq \frac{-\alpha_{m_f}}{2}, \delta \leq 0$$

$$\Rightarrow \alpha_{m_f} \geq -2\alpha_{m_0} \tag{54}$$

Using (4), (8) in (54) implies

$$\alpha_{m_f} \in [-2\alpha_{m_0}, 0] \tag{55}$$

■

PROPOSITION 2 The design constraint

$$\sigma_{\max} \geq -\frac{\alpha_{m_f}^2}{4(\alpha_{m_f} + \alpha_{m_0})}$$

governs the feasible set of $\sigma_{\max}$ for the proposed guidance law to achieve all impact angles in the range

$$\alpha_{m_f} \in [-\pi, -2\alpha_{m_0})$$

while using a bounded lateral acceleration.

PROOF Squaring (50) and considering positive values of δ implies

$$\left((\beta + 2) + \frac{4\alpha_{m_0}}{\alpha_{m_f}}\right)^2 \leq \beta^2 + 4\beta\frac{\alpha_{m_0}}{\alpha_{m_f}} \tag{56}$$

which upon further simplification results in

$$1 + 4\left(\frac{\alpha_{m_0}}{\alpha_{m_f}}\right)^2 + 4\left(\frac{\alpha_{m_0}}{\alpha_{m_f}}\right) \leq -\beta\frac{\alpha_{m_0}}{\alpha_{m_f}} - \beta$$

$$\Rightarrow \beta \leq -\frac{1 + 4\left(\frac{\alpha_{m_0}}{\alpha_{m_f}}\right)^2 + 4\left(\frac{\alpha_{m_0}}{\alpha_{m_f}}\right)}{1 + \frac{\alpha_{m_0}}{\alpha_{m_f}}} \tag{57}$$

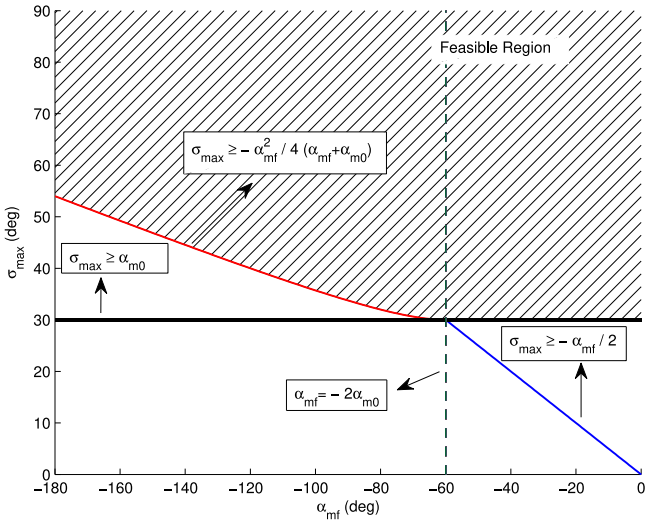

Fig. 3. Feasible solution in $(\alpha_{m_f} - \sigma_{\max})$ design space, $\alpha_{m_0} = 30^\circ$.

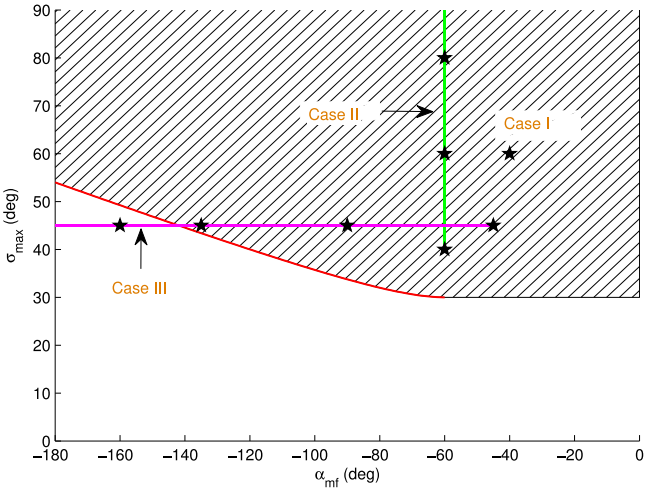

Fig. 4. Sample simulation points in the design space for $\alpha_{m_0} = 30^\circ$.

Using (30) in (57)

$$\frac{4(\sigma_{\max} - \alpha_{m_0})}{\alpha_{m_f}} \leq -\frac{\alpha_{m_f}^2 + 4\alpha_{m_0}^2 + 4\alpha_{m_0}\alpha_{m_f}}{\alpha_{m_f}(\alpha_{m_f} + \alpha_{m_0})}$$

$$\Rightarrow \sigma_{\max} \geq -\frac{\alpha_{m_f}^2}{4(\alpha_{m_f} + \alpha_{m_0})}, \delta > 0 \tag{58}$$

Using (51) in (58)

$$(\beta + 2) + \frac{4\alpha_{m_0}}{\alpha_{m_f}} > 0 \tag{59}$$

Also, using (30) in (59) yields

$$\frac{4(\sigma_{\max} - \alpha_{m_0})}{\alpha_{m_f}} + 2 + \frac{4\alpha_{m_0}}{\alpha_{m_f}} > 0 \tag{60}$$

$$\Rightarrow \sigma_{\max} < \frac{-\alpha_{m_f}}{2} \tag{61}$$

Finally, using (4), (8), and (22), (58) holds for all

$$\alpha_{m_f} \in [-\pi, -2\alpha_{m_0}) \tag{62}$$

■

Considering a launch angle of $\alpha_{m_0} = 30^\circ$, a sample design space satisfying the bounded terminal lateral acceleration is presented in Fig. 3. The design constraints governed by (22), (53), and (58) are depicted in black, blue, and red colors, respectively. The dashed green line denotes the condition $\alpha_{mf} = -2\alpha_{m0}$, which acts as a partition between the two design constraints represented in (53) and (58), respectively. The hatched area in the figure shows the feasible region in $(\alpha_{m_f} - \sigma_{\max})$ design space.

V. SIMULATION RESULTS

Numerical simulations are carried out considering a constant speed and a realistic missile model with given thrust and aerodynamic characteristics. The guidance law of (9) is used where the guidance gains are obtained using (33) and (34). The initial position of missile and the target are chosen as $(x_{m_0},\ y_{m_0}) = (0, 0)$ and $(x_t,\ y_t) = (5000\text{ m}, 0)$, respectively. All simulations are terminated for a miss distance $R < 0.1$ m. This section also includes a qualitative comparative study with existing works.

A. Constant Speed Missile Model

A missile with speed $V_m = 300$ m/s together with an initial heading of $\alpha_{m_0} = 30^\circ$ is considered. Satisfying the terminal lateral acceleration boundedness constraint, the feasible $(\alpha_{m_f} - \sigma_{\max})$ region for launch angle $\alpha_{m_0} = 30^\circ$ was presented in Fig. 3. Fig. 4 considers that feasible region and marks design pairs corresponding to subsequent case studies.

1) *Case I. Sample Simulation With $\sigma_{max} = 60^\circ$:* With the given initial conditions, a desired impact angle of $\alpha_{m_f} = -40^\circ$ along with the maximum look-angle $\sigma_{\max} = 60^\circ$ is considered. The impact angle and the maximum look-angle information is used in (33) and (34) to obtain the guidance gains k_1 and k_2 as -2.6213 and 12.5229, respectively. The missile trajectory is plotted in Fig. 5(a) showing successful interception with the desired impact angle. Lateral acceleration history is presented in Fig. 5(b). It can be seen that lateral acceleration is bounded. The look-angle variation is shown in Fig. 5(c) wherein the maximum value satisfies the given limit of 60°. Fig. 5(d) shows the missile heading profile. The variation in effective navigation gain $(N(t) = k_1 - k_2\theta)$ is plotted in Fig. 5(e), which shows that the gain attains a value greater than 2 in the terminal phase of the engagement. In addition, in this case, the effective navigation gain takes a negative value at the beginning of engagement. This facilitates greater shaping of the trajectory to achieve the desired impact angle while satisfying the maximum field-of-view limit. Fig. 5(f) shows the line-of-sight rate variation with respect to effective navigation gain. It is noteworthy that the magnitude of line-of-sight rate strictly decreases $\forall t : N(t) > 2$.

2) *Case II. Given Impact Angle With Different Seeker Field-of-View Limits:* Simulations are performed for $\alpha_{m_f} = -60^\circ$ with different seeker field-of-view limits

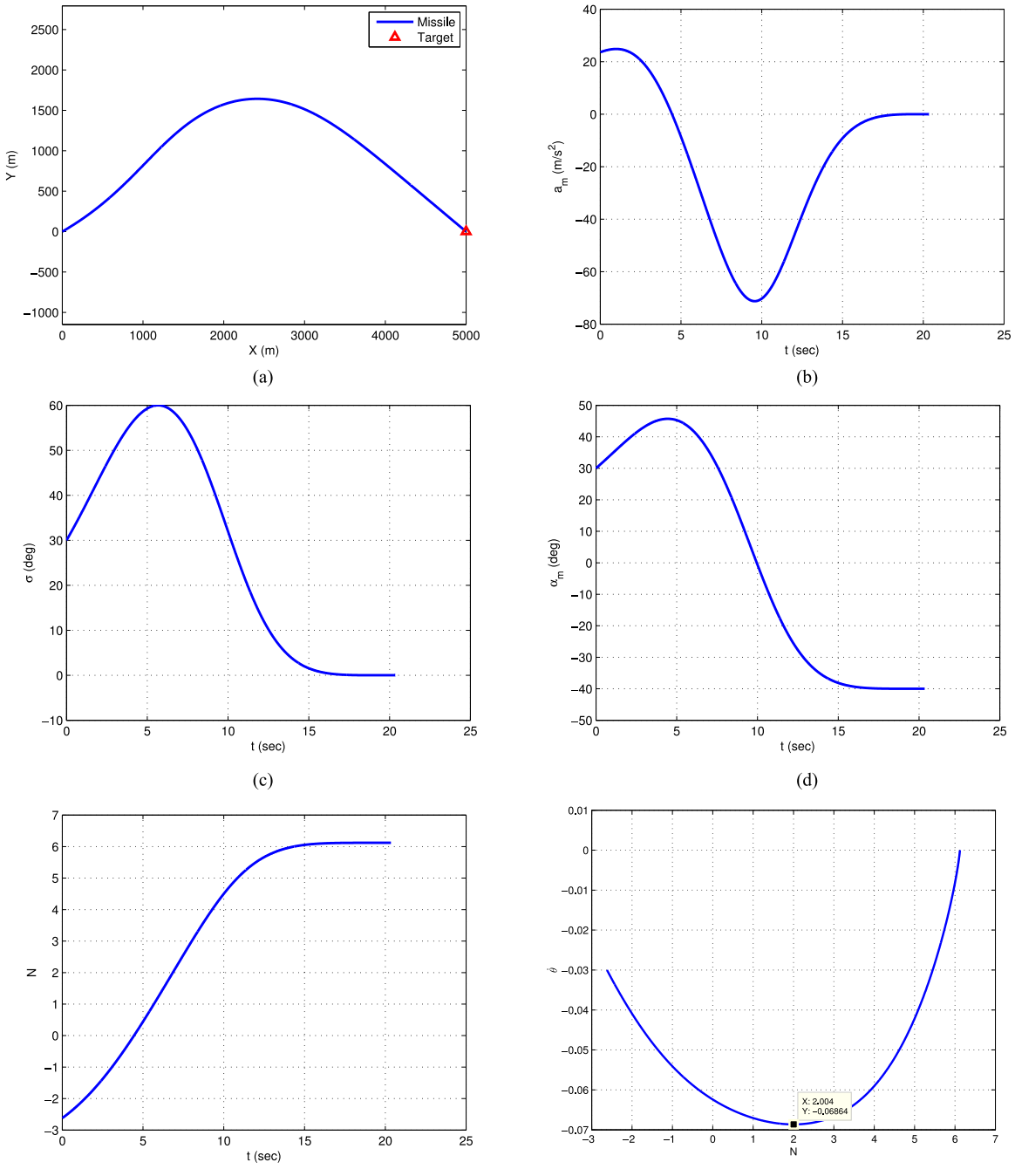

Fig. 5. Results for Case I: Sample scenario with $\alpha_{m_0} = 30^\circ$, $\sigma_{\max} = 60^\circ$, $\alpha_{m_f} = -40^\circ$.
(a) Missile trajectory. (b) Lateral acceleration history. (c) Look-angle variation. (d) Missile heading. (e) Variation in effective navigation gain.
(f) Line-of-sight rate variation with N.

$\sigma_{\max} = 40$, 60, and 80°, respectively. Fig. 6(a) shows missile trajectories with impacts along the desired direction. Lateral acceleration histories are plotted in Fig. 6(b). Since all the sample points for this case lie inside the feasible region as shown in Fig. 4, the corresponding lateral accelerations are bounded. The look-angle variations are plotted in Fig. 6(c) satisfying the respective seeker field-of-view limits. Fig. 6(d) shows variations in effective navigation gains with time. Results highlight the capability of proposed guidance law in achieving a desired impact angle while incorporating different seeker field-of-view limits.

3) *Case III. Different Impact Angles Using a Given Seeker Field-of-View:* With $\sigma_{\max} = 45^\circ$, this case considers multiple impact angles $\alpha_{m_f} \in [-\pi, 0]$. Trajectories for $\alpha_{m_f} = [-45, -90, -135, -160]^\circ$ are shown in Fig. 7(a) depicting the desired interception. Fig. 7(b) plots the lateral acceleration histories wherein the variation is bounded for

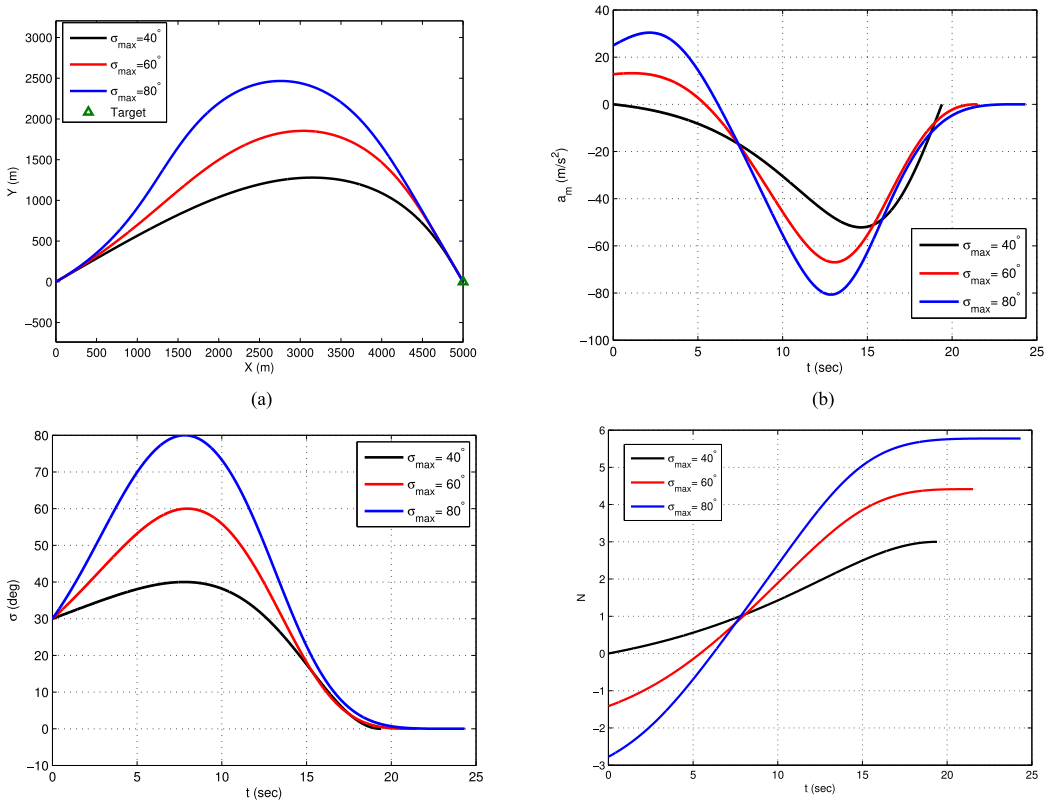

Fig. 6. Results for Case II: $\alpha_{m_0} = 30^\circ$, $\sigma_{\max} = [40,\ 60,\ 80]^\circ$, $\alpha_{m_f} = -60^\circ$. (a) Missile trajectories. (b) Lateral acceleration histories. (c) Look-angle profiles. (d) Effective navigation gains variations.

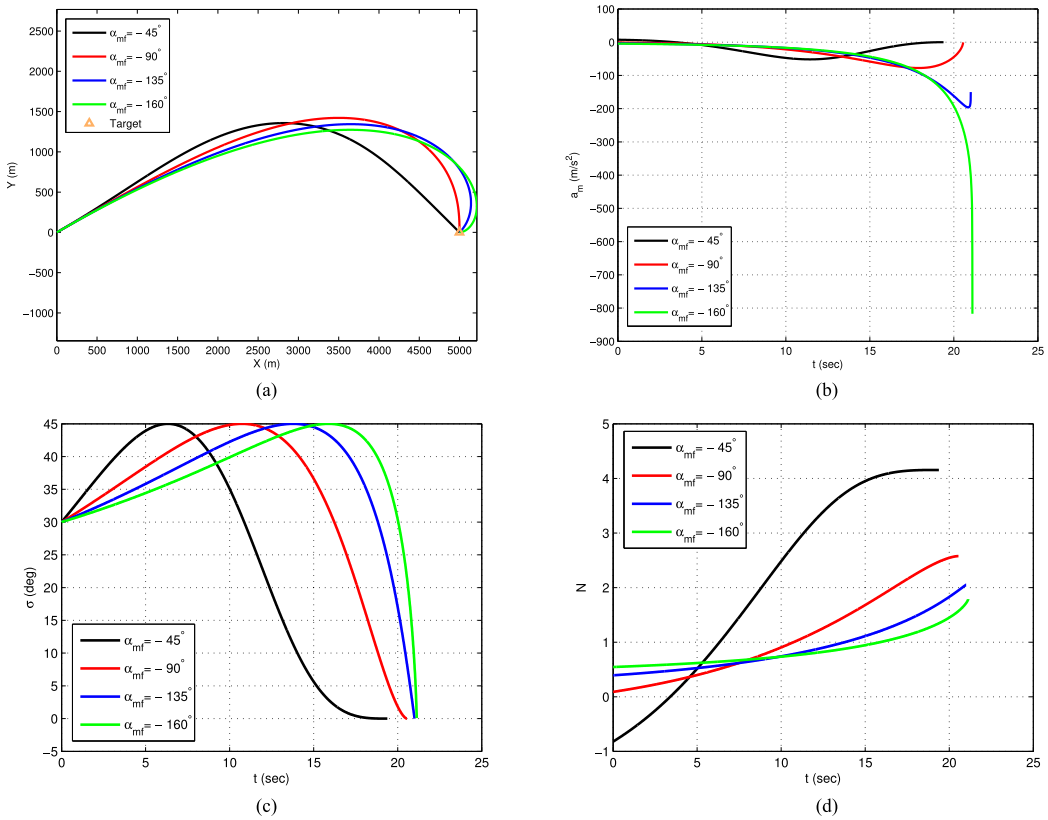

Fig. 7. Results for Case III: $\alpha_{m_0} = 30^\circ$, $\sigma_{\max} = 45^\circ$, $\alpha_{m_f} = [-45, -90, -135, -160]^\circ$. (a) Missile trajectories. (b) Lateral acceleration histories. (c) Look-angle profiles. (d) Effective navigation gain variations.

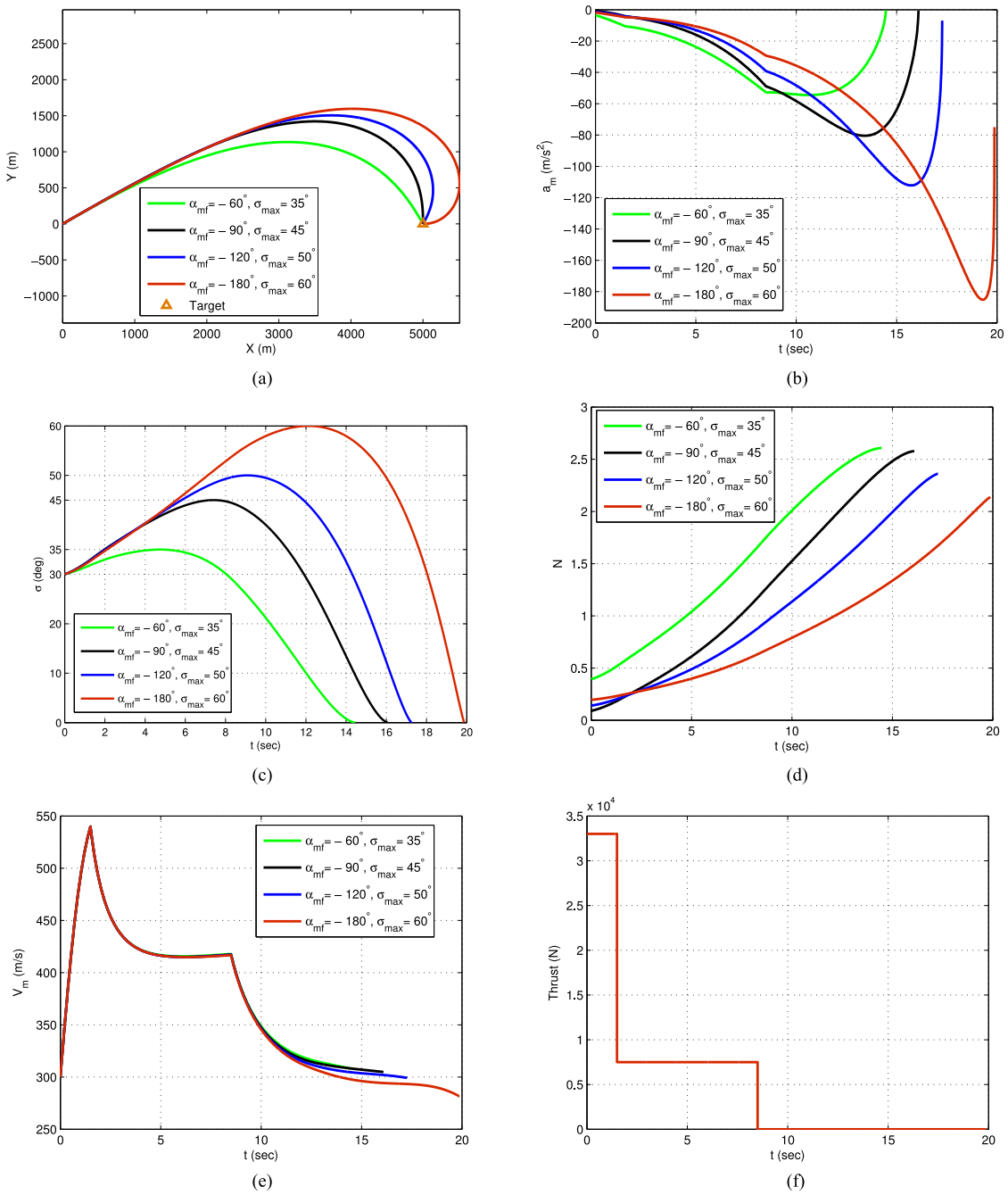

Fig. 8. Results for Case IV: Simulations for realistic missile model. (a) Missile trajectories. (b) Lateral acceleration histories. (c) Look-angle profiles. (d) Effective navigation gain variations. (e) Missile speed profiles. (f) Thrust profile.

$\alpha_{m_f} = [-45, -90, -135]^\circ$. For $\alpha_{m_f} = -160^\circ$, as shown in Fig. 4, the design pair $(\alpha_{m_f}, \sigma_{\max})$ is outside the feasible region, and hence the terminal lateral acceleration goes unbounded. Corresponding look-angle profiles satisfying the design constraints are shown in Fig. 7(c). Fig. 7(d) plots the variation in effective navigation gains with respect to time. It can be noted that for $\alpha_{m_f} = -160^\circ$, the effective navigation gain increases with time, however, it attains a final value $N(t_f) < 2$. Using (58) for $\alpha_{m_f} = -160^\circ$ leads to $\sigma_{\max} \geq 49.23^\circ$, which is not satisfied for the considered choice of $\sigma_{\max}$.

B. Realistic Simulations

With the same initial conditions as given for the constant speed model, simulations are carried out considering a realistic missile model. Assuming flat, nonrotating Earth, the equations of motion can be expressed as

$$\dot{x}_m = V_m \cos \alpha_m \tag{63}$$

$$\dot{y}_m = V_m \sin \alpha_m \tag{64}$$

$$\dot{V}_m = \frac{T - D}{m} - g \sin \alpha_m \tag{65}$$

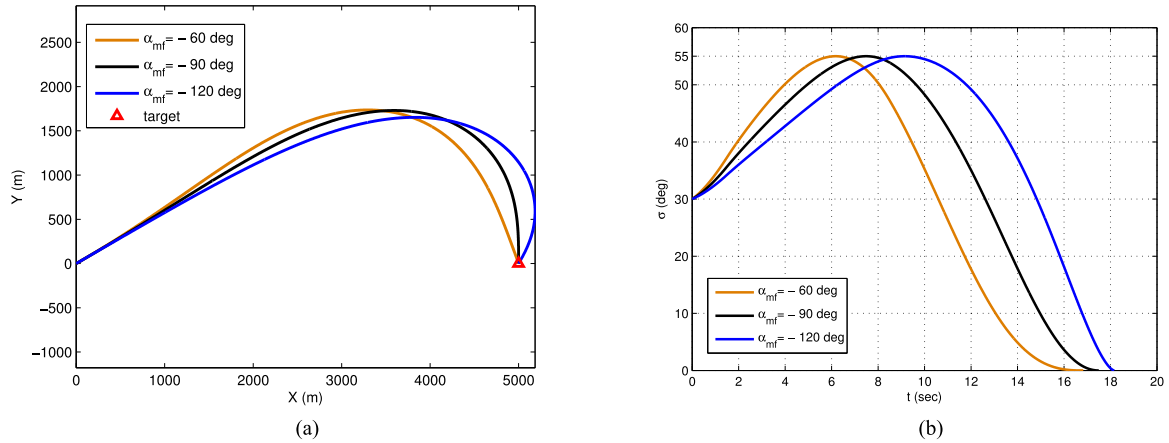

(a) (b)

Fig. 9. Results for Case IV: Simulations with practical field-of-view limit. (a) Missile trajectories. (b) Look-angle profiles.

$$\dot{\alpha}_m = \frac{a_m - g\cos\alpha_m}{V_m} \tag{66}$$

where x_m, y_m, m, T, D, and g denote downrange, altitude, missile mass, thrust, drag, and the acceleration due to gravity, respectively. The vehicle mass, thrust, and aerodynamic parameters are borrowed from [25], which are listed in Appendix. To compensate for the effect of gravity, the original guidance command (9) is augmented as

$$a_m = (k_1 - k_2\theta)\dot{\theta} V_m + g\cos\alpha_m \tag{67}$$

1) *Case IV. Simulations With Realistic Missile Model:* This case considers impact angles $\alpha_{m_f} = [-60, -90, -120, -180]^\circ$ with respective seeker's field-of-view limits as $\sigma_{\max} = [35,\ 45,\ 50,\ 60]^\circ$. All design pairs $(\alpha_{m_f}, \sigma_{\max})$ are chosen from within the feasible region shown in Fig. 4. Fig. 8(a) plots trajectories intercepting the target with desired impact angles. Presenting a bounded variation, lateral acceleration histories are plotted in Fig. 8(b). Corresponding look-angle profiles are shown in Fig. 8(c), which abide by the respective limits. Fig. 8(d) plots the variation in effective navigation gains with respect to time. Missile speed and thrust profiles are shown in Fig. 8(e) and (f), respectively.

In the proposed guidance structure, the maximum field-of-view is a design input to the feedback guidance law. The guidance gains are determined by equating the maximum look-angle on the trajectory to the specified design input. In practice, this design input can be readily chosen considering a realistic maximum limit accounting for any disturbances. To illustrate this aspect, additional simulations are carried out for achieving impact angles, $\alpha_{m_f} = [-60, -90, -120]^\circ$ with the maximum field-of-view limit, $\sigma_{\max} = 55^\circ$, which accounts for a 5° safety margin with respect to the actual maximum look-angle limit of 60°. Fig. 9(a) plots the missile trajectories satisfying the desired impact angles. As shown in Fig. 9(b), the look-angle profiles abide by the practical field-of-view limit. Applicability of proposed guidance method for the realistic case can be understood by investigating the nature of the guided trajectory. Using (1), (2), and (17), the spatial trajectory is governed by

$$\frac{1}{R}\frac{dR}{d\theta} = \cot\left((k_1 - 1)\theta - \frac{k_2\theta^2}{2} + \alpha_{m_0}\right)$$
$$\Rightarrow \int \frac{dR}{R} = \int \cot\left((k_1 - 1)\theta - \frac{k_2\theta^2}{2} + \alpha_{m_0}\right) d\theta \tag{68}$$

Though (68) cannot be solved in a closed form, it can be seen that the spatial trajectory is independent of missile speed. Hence, the proposed guidance law can be readily applied in realistic scenarios.

C. Robustness to Uncertainties

A robustness study is performed considering an uncertainty in modeling the drag coefficient. The uncertainty in drag coefficient, δC_{d0} is chosen as a random variable with a uniform distribution as $\delta C_{d0} \in [-0.002,\ 0.002]$. In addition, an uncompensated first-order autopilot dynamics is considered with a time constant, $\tau = 0.1$ s.

Table I summarizes the Monte Carlo simulation results for 500 runs. For a launch angle of $\alpha_{m_0} = 30^\circ$, three scenarios with different combinations are chosen as $(\alpha_{m_f}, \sigma_{\max}) = [(-60,\ 45), (-90,\ 60), (-180,\ 90)]$. Results show very small to negligible errors in impact angle and maximum look-angle limits considered for the study.

D. Comparison Studies

A qualitative comparison is carried out with existing guidance methods addressing the problem at hand. The methods are compared with respect to information needed to implement the guidance logic, nature and number of guidance parameters, and additional bias or switch requirements. Table II presents detailed results of the comparison. It can be seen that the proposed method offers the simplest solution for the problem. The method requires only two guidance gains k_1 and k_2, does not rely on numerical routines for guidance gain computations, and can be easily implemented with bearings information of the target. In addition, unlike [14], [15], [18], and [19], the proposed guidance neither uses switching nor any additional bias in the guid-

TABLE I
Monte Carlo Simulation Study: $\alpha_{m_0} = 30^\circ$ and $\tau = 0.1$ s

Scenarios	Impact angle (α_{m_f})	Field-of-View limit ($\sigma_{\max}$)	Standard Deviation (α_{m_f})	Mean (α_{m_f})	Standard Deviation ($\sigma_{\max}$)	Mean ($\sigma_{\max}$)
1	-60°	45°	-0.0009°	-59.8322°	0.0013°	45.4839°
2	-90°	60°	-0.0031°	-89.8046°	0.0016°	60.6870°
3	-180°	90°	-0.0047°	-179.7847°	0.007°	90.4267°

TABLE II
Qualitative Comparison With Existing Works

Guidance methods	Information needed	Guidance parameters	Guidance computations	Switching or additional bias
Ref. [14]	Target bearing	2: One guidance gain each for midcourse and terminal phase, respectively	Numerical routine for computing gains	Required
Ref. [15]	Target bearing	3: Navigation gain, bias magnitude, and time constant for the exponential bias profile	Closed-form equation for the guidance command and bias terms	Required
Ref. [18]	Target range and bearing	5: Two for the sliding surface, and additional three for the guidance command	Closed-form equation for the guidance command	Required
Ref. [19]	Target range	2: Switching ranges between three guidance phases	Closed-form relations for three phase guidance command, Switching ranges are derived using a numerical routine	Required
Ref. [22]	Target bearing	3: Two user defined parameters for sliding surface variable, and an additional one included in the guidance command	Closed-form equations for the sliding surface and the guidance command	Not required
Proposed method	Target bearing	2: Guidance gains, k_1 and k_2	Closed-form equations (9), (33), and (34) governing the guidance command and gains, respectively	Not required

ance command and hence generates smooth lateral acceleration profile. Limitations of the proposed method include a small and well-defined infeasible region in ($\alpha_{m_f} - \sigma_{\max}$) space [see (58)] for imposing a bounded terminal lateral acceleration constraint. However, as also illustrated in Fig. 4, that constraint leads to a reduced feasible $\sigma_{\max}$ range only for impact angles $\alpha_{m_f} < -2\alpha_{m_0}$ [see (62)].

VI. CONCLUSION

A two-gain feedback guidance law is investigated for achieving desired impact angles with missile seeker's field-of-view limits against stationary targets. Analyzing the look-angle profile, closed-form expressions of the guidance gains are derived satisfying the impact angle and maximum look-angle of the seeker. Target interception is guaranteed by deducing a strictly decreasing heading error profile in the terminal phase of the engagement. Ascertaining terminal lateral acceleration boundedness, a feasible implementable region is deduced in impact angle-maximum look-angle design space. Numerical simulations are performed considering a kinematic and realistic missile model. A comparison with existing methods highlights that the proposed guidance law does not require switching or additional bias terms in the guidance command. Amongst all such methods, the proposed one offers the simplest form of guidance command along with easily computable closed-form guidance gains.

APPENDIX
REALISTIC VEHICLE MODEL

A. Drag Model

The drag force acting on vehicle can be expressed as

$$D = \frac{1}{2}\rho V_m^2 S C_d \tag{69}$$

where ρ and C_d denote the atmospheric density and the coefficient of drag force, respectively. The reference area is taken as $S = 1$ m^2. Assuming negligible induced drag, the drag coefficient is governed by

$$C_d = \begin{cases} 0.02 & M < 0.93 \\ 0.02 + (M - 0.93) & M < 1.03 \\ 0.04 + 0.06(M - 1.03) & M < 1.10 \\ 0.0442 - 0.07(M - 1.10) & M \geq 1.10 \end{cases}$$

where M is the Mach number defined as

$$M = \frac{V_m}{a} = \frac{V_m}{\sqrt{\gamma \bar{R} T_{\text{emp}}}}$$

where a is the speed of sound, γ is the adiabatic index of air, and $\bar{R}$ is the specific gas constant.

B. Vehicle Properties

Thrust of the vehicle is given as

$$T = \begin{cases} 33000 & 0 \le t \le 1.5\,\text{s} \\ 7500 & 1.5 \le t \le 8.5\,\text{s} \\ 0 & 8.5 \le t\,\text{s} \end{cases}$$

Variation in mass of the vehicle with time is given as

$$m = \begin{cases} 135 - 14.53t & 0 \le t \le 1.5\,\text{s} \\ 113.205 - 3.31(t - 1.5) & 1.5 \le t \le 8.5\,\text{s} \\ 90.035 & 8.5 \le t\,\text{s} \end{cases}$$

C. Atmospheric Properties

Atmospheric density variation with altitude (h) is considered as

$$\rho(h) = 1.15579 - 1.058 \times 10^{-4} h + 3.725 \times 10^{-9} h^2 - 6 \times 10^{-14} h^3$$

where $h \in [0,\ 20\,000]$ m.

Temperature variation with altitude (h) is expressed as

$$T_{\text{emp}} = \begin{cases} 288.16 - 0.0065h\ \text{K} & h \le 11\,000\ \text{m} \\ 216.66\ \text{K} & h > 11\,000\ \text{m} \end{cases}$$

K stands for Kelvin (unit of temperature).

REFERENCES

[1] M. Kim and K. V. Grider
Terminal guidance for impact attitude angle constrained flight trajectories
IEEE Trans. Aerosp. Electron. Syst., vol. AES-9, no. 6, pp. 852–859, Nov. 1973.

[2] T. L. Song, S. J. Shin, and H. Cho
Impact angle control for planar engagements
IEEE Trans. Aerosp. Electron. Syst., vol. 35, no. 4, pp. 1439–1444, Oct. 1999.

[3] C. K. Ryoo, H. Cho, and M. J. Tahk
Optimal guidance law with terminal impact angle constraint
J. Guid., Control, Dyn., vol. 28, no. 4, pp. 724–732, Jul./Aug. 2005.

[4] C. K. Ryoo, H. Cho, and M. J. Tahk
Time-to-Go weighted optimal guidance with impact angle constraints
IEEE Trans. Control Syst. Technol., vol. 14, no. 3, pp. 483–492, May 2006.

[5] H. B. Oza and R. Padhi
Impact-angle-constrained suboptimal model predictive static programming guidance of air-to-ground missiles
J. Guid., Control, Dyn, vol. 35, no. 1, pp. 153–164, Jan./Feb. 2012.

[6] V. Shaferman and T. Shima
Linear quadratic guidance laws for imposing a terminal intercept angle
J. Guid., Control, Dyn., vol. 31, no. 5, pp. 1400–1412, Sep./Oct. 2008.

[7] T. Shima
Intercept angle guidance
J. Guid., Control, Dyn., vol. 34, no. 2, pp. 484–492, Mar./Apr. 2011.

[8] S. R. Kumar, S. Rao, and D. Ghose
Sliding-mode guidance and control for all-aspect interceptors with terminal angle constraints
J. Guid., Control, Dyn., vol. 35, no. 4, pp. 1230–1246, Jul./Aug. 2012.

[9] P. Lu, D. B. Doman, and J. D. Schierman
Adaptive terminal guidance for hypervelocity impact in specified direction
J. Guid., Control, Dyn., vol. 29, no. 2, pp. 269–278, Mar./Apr. 2006.

[10] A. Ratnoo and D. Ghose
Impact angle constrained interception of stationary targets
J. Guid., Control Dyn., vol. 31, no. 6, pp. 1817–1822, Nov./Dec. 2008.

[11] K. S. Erer and O. Merttopcuoglu
Indirect impact-angle-control against stationary targets using biased pure proportional navigation
J. Guid., Control, Dyn., vol. 35, no. 2, pp. 700–704, Mar./Apr. 2012.

[12] A. Ratnoo
Nonswitching guidance law for trajectory shaping control
J. Guid., Control, Dyn., vol. 40, no. 10, pp. 2721–2728, Oct. 2017.

[13] K. S. Erer, R. Tekin, and M. K. Ozgoren
Look angle constrained impact angle control based on proportional navigation
In *Proc. AIAA Guid., Navig., Control Conf.*, Jan. 2015, pp. 2015–0091.

[14] R. Tekin and K. S. Erer
Switched-gain guidance for impact angle control under physical constraints
J. Guid., Control, Dyn., vol. 38, no. 2, pp. 205–216, Feb. 2015.

[15] T. H. Kim, B. J. Park, and M. J. Tahk
Bias-shaping method for biased proportional navigation with terminal-angle constraint
J. Guid., Control, Dyn., vol. 36, no. 6, pp. 1810–1815, Nov./Dec. 2013.

[16] C. K. Ryoo, H. Cho, and M. J. Tahk
Biased PNG with terminal-angle constraint for intercepting nonmaneuvering targets under physical constraints
IEEE Trans. Aerosp. Electron. Syst., vol. 53, no. 3, pp. 1562–1572, Jun. 2017.

[17] A. Ratnoo
Analysis of two-stage proportional navigation with heading constraints
J. Guid., Control, Dyn., vol. 39, no. 1, pp. 156–164, Jan. 2016.

[18] S. He and D. Lin
A robust impact angle constraint guidance law with seeker's field-of-view limit
Trans. Inst. Meas. Control, vol. 37, no. 3, pp. 317–328, Jun. 2014.

[19] B. G. Park, T. H. Kim, and M. J. Tahk
Optimal impact angle guidance law considering the seeker's field-of-view limits
Proc. Inst. Mech. Eng., Part G: J. Aerosp. Eng., vol. 227, no. 8, pp. 1347–1364, Jun. 2012.

[20] B. G. Park, T. H. Kim, and M. J. Tahk
Range-to-Go weighted optimal guidance with impact angle constraint and seekers look angle limits
IEEE Trans. Aerosp. Electron. Syst., vol. 52, no. 3, pp. 1241–1256, Jun. 2016.

[21] Z. Yang, H. Wang, and D. Lin
Time-varying biased proportional guidance with seeker's field-of-view
Int. J. Aerosp. Eng., vol. 2016, pp. 1–11, 2016.

[22] H. G. Kim, J. Y. Lee, and H. J. Kim
Look angle constrained impact angle control guidance law for homing missiles with bearings-only measurements
IEEE Trans. Aerosp. Electron. Syst., vol. 54, no. 6, pp. 3096–3107, Dec. 2018.

[23] Y. R. Sharma and A. Ratnoo
Guidance law for mimicking short range ballistic trajectories
Proc. Inst. Mech. Eng., Part G: J. Aerosp. Eng., pp. 1–15, Dec. 2018.

[24] N. A. Shneydor
Missile Guidance and Pursuit, 1st ed. Chichester, U.K.: Ellis Horwood Publishing, 1998, pp. 101–105, Ch. 5.

[25] P. E. Kee, L. Dong, and C. J. Siong
Near optimal midcourse guidance law for flight vehicle
In *Proc. AIAA Aerosp. Sci. Meeting Exhibit*, Jan. 1998, p. 583.

Yash Raj Sharma received the Bachelor's degree in aeronautical engineering from the FGIET Engineering College, Raebareli, India, in 2016, and the M.Tech. (Research) degree in aerospace engineering from the Indian Institute of Science, Bangalore, India, in 2018.

He is currently a Research Associate with Autonomous Vehicles Laboratory, Department of Aerospace Engineering, Indian Institute of Science. His research interests include guidance and control of autonomous vehicles, and flight and space mechanics.

Ashwini Ratnoo received the B.E. degree in electrical engineering from the MBM Engineering College, Jodhpur, India, in 2003, and the M.E. and Ph.D. degrees in aerospace engineering from the Indian Institute of Science, Bangalore, India, in 2005 and 2009, respectively.

During 2009–2012, he was a Postdoctoral Researcher with the Aerospace Engineering Department, Technion-Israel Institute of Technology, Haifa, Israel. He is currently an Associate Professor with the Aerospace Engineering Department, Indian Institute of Science, Bangalore, India. His research interests include guidance and control of autonomous vehicles.

Dr. Ratnoo is a Senior Member of AIAA.